Microscopic Equations-of-State for Hydrocarbon Fluids: Effect of Attractions and Comparison with Polyethylene Experiments

John G. Curro,*,† Arun Yethiraj,‡ Kenneth S. Schweizer,‡ John D. McCoy,§ and Kevin G. Honnell‖

Sandia National Laboratories, Albuquerque, New Mexico 87185, Department of Materials Science & Engineering and Materials Research Laboratory, University of Illinois, Urbana, Illinois 61801, Materials & Metallurgical Engineering Department, New Mexico Institute of Mining & Technology, Socorro, New Mexico 87801, and Phillips Petroleum Company, Bartlesville, Oklahoma 74006

Received October 26, 1992; Revised Manuscript Received February 2, 1993

ABSTRACT: Microscopic equations-of-state are developed for *n*-alkanes and polyethylene based on the polymer reference interaction site model (PRISM) integral equation theory and a generalized Flory approach. The molecules are modeled as a series of overlapping spheres (methylene groups) with constant bond length and bond angles; internal rotations are accounted for by the rotational isomeric state approximation. The interaction between sites on different molecules is taken to be of the Lennard-Jones form. The thermodynamic properties of the fluid are obtained via standard perturbation theory in which the potential is divided into a repulsive reference system and an attractive perturbation. The reference system is approximated by a hard-core repulsion in which the hard-sphere diameter $d(T)$ is estimated for polyethylene from wide-angle X-ray scattering experiments. The PRISM theory is used to calculate the hard-sphere chain contribution to the equation-of-state by three different thermodynamic routes: (1) integrating the compressibility, (2) evaluating the density profile at a hard wall, and (3) using a hard-sphere "charging" method analogous to the virial approach in monatomic liquids. The generalized Flory dimer (GFD) theory is used to obtain a fourth equation-of-state for the hard-sphere chains. The attractive perturbation is treated with first-order perturbation theory, making use of the radial distribution function $g_0(r)$ of the reference system. The various equations-of-state presented differ in the route to the hard-chain pressure; PRISM is used in all cases to treat the attractions. Excellent agreement for the equation-of-state is found between the hybrid GFD/PRISM calculations and molecular dynamics simulations of *n*-butane and experimental pressure–volume–temperature (*PVT*) measurements on polyethylene melts. The compressibility and charging routes predict pressures which are too low and too high, respectively, for polyethylene. The wall route yields pressures in good agreement at experimental densities but predicts a melt which is too compressible.

I. Introduction

A microscopic description of the equation-of-state of polymer liquids is a well-known problem which has been investigated by many workers.[1-8] Early polymer equation-of-state theories have necessarily consisted of lattice, cell, or hole model descriptions. Although approaches such as those due to Simha and Somcynsky[2] or Sanchez and Lacombe[3] work quite well when compared to experimental data, they are based on qualitatively useful but quantitatively undefined parameters such as free volume and number of external degrees of freedom. It is not obvious how these parameters are related to the molecular architecture of the actual polymer chains. More recently, equation-of-state theories for tangent hard-sphere chains[4-7] and square-well chains[8] have been developed in continuous space. The idealized nature of these models does not allow them to reliably predict actual experimental data; however, computer simulations can be used to test their validity. In the present investigation, we will focus on calculating the equation-of-state of polyethylene and alkane liquids in continuous space. In order to compare with experimental pressure–volume–temperature (*PVT*) data, we model the chains with a realistic backbone structure (rotational isomeric state model) interacting with realistic intermolecular potentials (Lennard-Jones).

Recently, integral equation techniques have been developed to calculate the intermolecular structure of polymer melts.[9-13] These methods are a generalization to polymers of the reference interaction site model (RISM theory) of Chandler and Andersen.[14-16] This new theory, which we call polymer RISM or PRISM theory, has also been expanded to allow both the intramolecular and intermolecular structure of homopolymer liquids to be determined in a self-consistent manner.[17] Extensions have also been made of the PRISM theory to binary blends.[18-23] Good agreement of the PRISM theory with molecular dynamics[17,24,25] and Monte Carlo[26] simulations was found for the radial distribution function of hard-core chain liquids. Comparisons have also been made between the structure factor for polyethylene melts obtained from the PRISM theory and X-ray scattering experiments of Narten and Habenschuss.[27,28] Remarkably good agreement was found by modeling the polyethylene as overlapping hard-sphere chains.

On the basis of these comparisons between simulation and experiment, it seems that the PRISM theory adequately describes the intermolecular structure of homopolymer liquids. The level of accuracy for polymers appears to be about the same as corresponding RISM calculations for small, rigid molecules as far as intermolecular structure or packing is concerned. A natural question to ask is, can the PRISM approach also be employed to calculate *thermodynamic* properties of polymer melts? In earlier work[7] Schweizer and Curro used PRISM theory to compute the equation-of-state for freely-jointed chains using a virial route to the pressure in which a superposition approximation was made for the three-body correlation function. The results were inconclusive, however, since the superposition approximation was later shown to be inaccurate.[29,30]

† Sandia National Laboratories.
‡ University of Illinois.
§ New Mexico Institute of Mining & Technology.
‖ Phillips Petroleum Co.

0024-9297/93/2226-2655$04.00/0

In a recent publication[31] (designated as paper 1) we reexamined this question by computing the equation-of-state of alkane chain liquids interacting with hard-core repulsions between intermolecular sites (methylene groups). In this study we calculated the equation-of-state from PRISM theory by three different routes and also from the generalized Flory dimer[4,5] (GFD) theory, suitably extended to overlapping hard-sphere chains. Unfortunately, since the PRISM theory is an approximate theory for intermolecular structure and the pressure is known to be an extremely sensitive function of $g(r)$, significantly different results for the hard-chain pressure are found from the three routes.

In the present investigation we continue this equation-of-state theme by considering polymer chains interacting with a Lennard-Jones potential. Our strategy will be to use our previous hard-sphere chain model as a reference system and then to include the effect of attractive interactions as a perturbation.[32] The hard-core diameter of the reference system is then chosen in an optimum fashion to match the continuous soft-core repulsion of the Lennard-Jones potential. These calculations can thus be compared with PVT experiments on polyethylene melts. It should be mentioned that recently Yethiraj and Hall[8b] calculated the equation-of-state of square-well chain fluids of $n = 4, 8$, and 16 units by using a GFD/PRISM approach. They found good agreement with computer simulations at meltlike densities.

An obvious difficulty in making comparisons to experimental data, in contrast to simulations, is the ambiguity that exists regarding the interatomic potentials. Assuming a Lennard-Jones form, a clean comparison with experiment is obscured by two adjustable parameters. In the present investigation, we eliminate one of these parameters by choosing the hard-core diameter to give agreement with the first peak in the experimental structure factor of polyethylene. We have some feeling for the magnitude of the remaining adjustable parameter, the depth of the attractive well, based on known values for short alkanes.[48]

We will begin by briefly reviewing the PRISM theory and its application to computing the hard-core polymer equation-of-state.[31] Our strategy for using these hard-core results, together with perturbation theory, to model Lennard-Jones interactions between methylene groups is also presented in section II. Numerical results for butane are presented in section III and compared with the simulations of Ryckaert and Bellemans.[33,34] Calculations for polyethylene by the various routes are also presented and critically compared with experimental PVT data. The paper concludes with a brief discussion in section IV.

II. Theory

The PRISM theory[9-13] is an extension to flexible polymers of the reference interaction site model of Chandler and Andersen[14-16] and has been discussed in detail previously.[10,11] In this approach, each polymer is taken to consist of a chain of spherically symmetric sites; intermolecular interactions occur only between these sites. The intersite direct correlation function $C(r)$ is related to the intersite radial distribution function $g(r)$ through a generalized Ornstein–Zernike equation. For long chains we can neglect end effects; consequently the correlations between any pair of intermolecular sites are taken to be the same regardless of their position along the chain. After the appropriate preaveraging over the intramolecular structure of the polymer molecule, the generalized Ornstein–Zernike equation becomes

$$\hat{h}(k) = \hat{\omega}(\mathbf{k})\,\hat{C}(\mathbf{k})\,\hat{\omega}(\mathbf{k}) + \rho_m\hat{\omega}(\mathbf{k})\,\hat{C}(\mathbf{k})\,\hat{h}(\mathbf{k}) = \hat{\omega}(\mathbf{k})\,\hat{C}(\mathbf{k})\,\hat{S}(\mathbf{k}) \quad (1)$$

where the carets denote Fourier transformation with respect to wavevector $\mathbf{k}$, $h(r)$ is the total correlation function defined as $h(r) = g(r) - 1$, and ρ_m is the monomer or site density. All the information about the intramolecular structure of the polymer molecules enters the theory through the function $\omega(r)$

$$\omega(r) = \frac{1}{N}\sum_{i,j}\omega_{ij}(r) \quad (2)$$

where the sum is extended over all intramolecular pairs of N repeat units per chain, and $\omega_{ij}(r)$ is the probability density that sites i and j are a distance r apart. $\hat{S}(\mathbf{k})$ is the structure factor defined as $\hat{\omega}(\mathbf{k}) + \rho_m\hat{h}(\mathbf{k})$. In general, the intramolecular probability function $\omega(r)$ and the intermolecular correlations $C(r)$ and $g(r)$ would have to be determined self-consistently. Although we have recently developed methods for dealing with this difficult self-consistent calculation,[17] for simplicity this self-consistency calculation will be avoided in the present paper. Instead, we make use of the Flory ideality hypothesis[35] which appears to be an excellent approximation in dense homopolymer melts based on SANS measurements and computer simulations. With this approximation, we can then calculate $\omega(r)$ from a separate single-chain calculation in which long-range, excluded-volume and many-body, medium-induced interactions are omitted. The Flory ideality hypothesis is expected to improve[17] in the case of real polymer chains such as polyethylene which, in contrast to freely jointed chains, have some stiffness which prevents local overlap of intramolecular chain segments.

Introduction of the $\omega(r)$ function appropriate to the particular polymer structure into the generalized Ornstein–Zernike equation above leads to a relation between intermolecular correlation functions $C(r)$ and $g(r)$. An additional *closure* relation is needed in order to uniquely solve for these functions. For hard-core interactions, we have the exact expression

$$h(r) = -1, \quad r < d \quad (3a)$$

resulting from the impenetrability of hard spheres of diameter d. On the basis of an analogy with the Percus–Yevick (PY) theory for hard spheres,[32] Chandler and Andersen suggested[14-16] the atomic-like closure

$$C(r) \cong 0, \quad r > d \quad (3b)$$

taken to be approximately valid outside the hard core. We have found this PY type closure to be accurate for the intermolecular structure of hard-sphere polymer chains by comparison with MD[17,24,25] and Monte Carlo[26] simulations, as well as, with experimental X-ray scattering experiments on polyethylene liquids.[27,28] Equations 1–3 then form a nonlinear integral equation for the intermolecular $g(r)$ of a homopolymer melt. This integral equation can be solved numerically by either a variational method[35] or an iterative approach.

Complications arise if the interaction potential contains an attractive branch. In the case of polymer blends, use of the atomic-like MSA closure for attractions leads to a nonclassical molecular weight dependence[19-22] of the critical temperature at variance with recent simulations[36] and SANS experiments.[37] Recent theoretical studies[38] suggest that atomic-like closures are not appropriate for attractive interactions in polymers and new molecular-

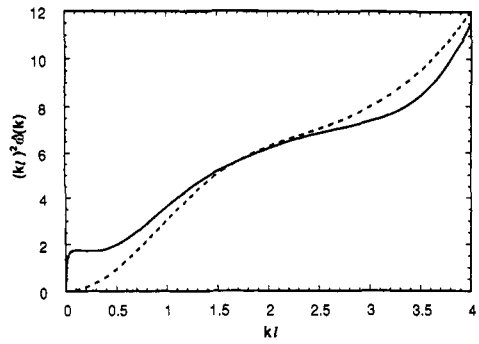

Figure 1. Intramolecular structure factor $\hat{\omega}(\mathbf{k})$ for n-butane (dashed curve) (d = 3.77 Å, T = 300 K) and polyethylene (solid curve) (d = 3.90 Å, T = 430 K, N = 6429) plotted in Kratky form.

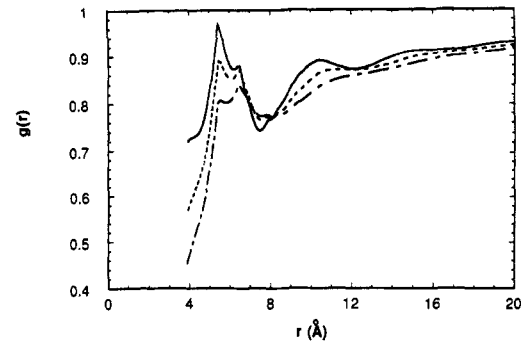

Figure 2. Intermolecular radial distribution function $g(r)$ computed for polyethylene (d = 3.90 Å, T = 430 K, N = 6429) using PRISM theory. The solid curve is for density $\rho_m d^3 = 2.2$, the short dashed curve for $\rho_m d^3 = 2.0$, and the dash-dot curve for $\rho_m d^3 = 1.8$.

based closures have been proposed. In the present work there is no difficulty in using the hard-core closure (eq 3b), since only the repulsive portion of the intermolecular potential is analyzed using integral equation theory; the contribution to the pressure due to the attractive tail of the potential will be accounted for by perturbation theory.

In paper 1 we modeled the methylene groups along the chain backbone of polyethylene as overlapping hard spheres of diameter d. The backbone structure of polyethylene was calculated using a rotational isomeric state approach[39] with bond length l, bond angle θ, and torsional rotational angles ϕ. The intramolecular structure factor $\hat{\omega}(\mathbf{k})$, the Fourier transform of $\omega(r)$ defined in eq 2, cannot be computed analytically for the rotational isomeric state model. In our previous studies on polyethylene[27,28,31] we estimated $\hat{\omega}(\boldsymbol{k})$ by treating the terms in eq 2 corresponding to the local structure exactly and approximating the long-range contributions.[39] The short-range structure is treated explicity by enumerating the rotational isomeric states for distances $|i - j| \leq 5$ along the backbone. Thus the pentane effect is included exactly. The $\hat{\omega}_{ij}(\mathbf{k})$ corresponding to distances $|i - j| \geq 6$ are approximately calculated from a semiflexible chain model, subject to the condition that the second and fourth moments of r_{ij} agree with the rotational isomeric state model. In the rotational isomeric state calculation the bond length was taken as 1.54 Å, the bond angle as 112°, and gauche states of ±120° relative to trans were used for polyethylene. A trans/gauche energy of 500 cal/mol and an additional gauche$^+$/gauche$^-$ energy of 2000 cal/mol was used. In the butane calculation, $\hat{\omega}(\mathbf{k})$ was evaluated exactly for the rotational potential, bond length, and bond angles employed by Ryckaert and Bellemans[33,34] in their simulations. The results for the continuous potential of butane were indistinguishable from a rotational isomeric state calculation with a trans/gauche energy of 700 cal/mol.

A plot of the intramolecular structure factor is shown in Figure 1 for both polyethylene and butane. Note that, in polyethylene, there appears a well-defined intermediate scaling regime in the range $0.1 < kl < 0.4$ for which $\hat{\omega}_{ij}(\mathbf{k}) \sim 1/(kl)^2$ expected for long chains. For butane no such scaling regime is observed. For the calculation of the equation-of-state, we expect all wavevector contributions to $\hat{\omega}(\mathbf{k})$ to be important.

The intermolecular radial distribution function has been obtained in paper 1 by solving eqs 1–3 using the intramolecular structure factors for polyethylene and butane. Representative $g(r)$'s are shown in Figure 2 for polyethylene melts at three different densities.

Having solved for the intermolecular structure, it is in principle possible to then obtain the thermodynamic properties of the melt. Because the PRISM theory for the structure is only approximate, the calculated thermodynamic functions depend on the particular statistical mechanical route used. In paper 1 three different routes were employed to extract the hard-core contribution to the pressure from the PRISM results: the compressibility, charging, and wall methods. In the compressibility route, one simply integrates the isothermal compressibility κ_T from zero density to the density of interest. The compressibility is related to the structure factor at zero wave vector according to $\rho_m k_B T \kappa_T = \hat{S}(0)$. The pressure can then be seen to be

$$\frac{\beta P}{\rho_m} = \frac{1}{\rho_m}\int_0^{\rho_m} \hat{S}^{-1}(0,\rho')\, d\rho' \qquad (4)$$

where $\beta = 1/k_B T$. The analog of the virial route for polyatomic liquids was put forth by Chandler[15] and consists of gradually turning on the hard-sphere diameter, starting from a point, as a charging parameter λ varies from 0 to 1. This charging procedure gives the Helmholtz free energy for a homopolymer fluid as

$$\frac{A - A_0}{V} = 2\pi\rho_m{}^2 d^3 k_B T \int_0^1 g^{(\lambda)}(\lambda d^+)\, \lambda^2\, d\lambda \qquad (5)$$

where A and A_0 are the free energies of the hard-core fluid and an ideal gas of chains, respectively, and $g^{(\lambda)}(\lambda d^+)$ is the contact value for $g(r)$ for a liquid comprised of interaction sites of hard-core diameter λd. The pressure is then obtained from eq 5 by numerical differentiation with respect to volume. In the monomeric fluid limit, eq 5 leads to the familiar virial formula for the pressure. Yet a third route to the pressure was utilized recently by Dickman and Hall[40] for extracting the pressure from Monte Carlo simulations and used by Yethiraj and Hall[41] in conjunction with PRISM theory. In this wall approach the pressure is simply related to the density of chain sites at a hard wall

$$\beta P/\rho_m = g_w(0) \qquad (6)$$

where $g_w(z)$ is the total site density profile in the direction perpendicular to the wall; the wall is impenetrable to the centers of the chain sites. Using the $g_w(z)$ predicted by PRISM theory, eq 6 was found to be accurate at high densities[41] but breaks down at low densities.

In paper 1 we extended the generalized Flory dimer (GFD) theory[4,5] of Hall, Dickman, and Honnell for tangent hard-sphere chains to the case of overlapping hard spheres, a model appropriate for alkanes, polyethylene, and other chain molecules. In this approach the pressure of a liquid composed of hard chains is approximately mapped onto a fluid of hard dimers and monomers. The compressibility factor $Z(N,\eta) \equiv \beta P/\rho_m$ of an N-mer fluid of monomer density ρ_m or packing fraction η is approximately related to the corresponding monomer and dimer compressibility

factors:

$$NZ(N,\eta) \cong 2(1 + Y_N)Z(2,\eta) - Y_N Z(1,\eta) \quad (7a)$$

where Y_N is related to $v_e(N)$, the volume excluded by an N-mer to a monomer, averaged over all conformations of the N-mer, i.e.

$$Y_N = \frac{v_e(N) - v_e(2)}{v_e(2) - v_e(1)} \quad (7b)$$

The Carnahan–Starling[42] and Tildesley–Streett[43] equations are used for $Z(1,\eta)$ and $Z(2,\eta)$, respectively. In paper 1 we showed that the identification of the monomer and dimer "reference" fluids whose compressibility factors appear in eq 7a is not unique. One way of obtaining the reference monomer and dimer fluids is to merely relax all the bonding constraints in the polymer fluid (GFD-A); since the packing fraction is kept constant, this results in a decrease in the site density of the monomer and dimer fluids from that of the polymer fluid. The second way of obtaining the reference monomer and dimer fluids is to require that both the packing fraction and the site density of the monomer and dimer fluids remain the same as in the polymer fluid (GFD-B); this results in the monomer and dimer molecules having different hard-core diameters than the polymer molecules. In paper 1 it was concluded that the GFD-B method was more appropriate (and more accurate) than the GFD-A and will therefore be employed in the present investigation.

In order to describe polyethylene, we represent the CH_2 groups as single sites interacting with a united atom potential of the Lennard-Jones form

$$v(r) = 4\epsilon[(\sigma/r)^{12} - (\sigma/r)^6] \quad (8)$$

where σ and ϵ are the usual Lennard-Jones parameters. In standard perturbation theory of liquids,[32] it is customary to divide the potential into a reference part $v_0(r)$ and a perturbative part $v_a(r)$. It is assumed that the intermolecular radial distribution function $g_0(r)$ can be calculated for the reference system with potential $v_0(r)$. A free energy expansion is then performed about the reference system, assuming that the perturbative potential $v_a(r)$ is small. To first order the Helmholtz free energy per unit volume is given by

$$A = A_0 + \frac{1}{2}\rho_m^2 \int g_0(r)\, v_a(r)\, d\vec{r} + \ldots \quad (9)$$

Two well-known perturbation approaches that have been applied to molecular fluids are the Barker–Henderson (BH) theory[44,45] and the Weeks–Chandler–Andersen (WCA) theory.[46] These two approaches differ in their choice of $v_0(r)$ and $v_a(r)$. For the BH theory, the reference and perturbative potentials are taken to be the repulsive and attractive branches of the Lennard-Jones potential, respectively.

$$\begin{aligned} v_0(r) &= v(r); \quad r \le \sigma \\ &= 0; \quad r > \sigma \end{aligned}$$

$$\begin{aligned} v_a(r) &= 0; \quad r \le \sigma \\ &= v(r); \quad r > \sigma \end{aligned} \quad (10)$$

The WCA theory uses the separation

$$\begin{aligned} v_0(r) &= v(r) + \epsilon; \quad r \le 2^{1/6}\sigma \\ &= 0; \quad r > 2^{1/6}\sigma \end{aligned}$$

$$\begin{aligned} v_a(r) &= -\epsilon; \quad r \le 2^{1/6}\sigma \\ &= v(r); \quad r > 2^{1/6}\sigma \end{aligned} \quad (11)$$

for which the perturbation varies more slowly than the BH perturbation over the range of r near the maximum in $g_0(r)$ for monatomic fluids. Because of the correlation hole effect[12] in polymeric fluids, the first peak is significantly smaller (see Figure 2 for polyethylene) and, depending on the density and chain length, may disappear altogether. As a consequence, the significant improvement in WCA over BH perturbation theory demonstrated in monatomic fluids may not carry over to polymer liquids.

In eqs 10 and 11 it can be seen that the reference potential $v_0(r)$ is a continuous, soft-core repulsion. It is customary to use a hard-core potential for the reference system and then to choose the hard-core diameter d in an optimum fashion to mimic the continuous repulsion. For the BH theory, this optimum hard core depends only on temperature.

$$d = \int_0^\infty \{1 - \exp[-\beta v_0(r)]\}\, dr \quad (12)$$

In the WCA theory d is calculated using a "blip" function technique. For the case of the Percus–Yevick, hard-sphere closure in eq 3b, d is chosen to satisfy

$$\int_0^d r^2 \exp[-\beta v_0(r)] C_0(r;d)\, dr + \int_d^\infty r^2 \{1 - \exp[-\beta v_0(r)]\} g_0(r;d)\, dr = 0 \quad (13)$$

where C_0 and g_0 are the direct correlation and radial distribution functions for the hard-core system with hard-core diameter d. Since both of these correlation functions are state-dependent functions, d in the WCA theory depends on both temperature and density, in contrast to the BH theory where d is only temperature dependent. As a result, the BH theory is much easier to implement than the WCA theory. In practice, we have found the difference in the d's predicted by eqs 12 and 13 to be quite small ($\sim$0.5%) for polyethylene melts. It should be mentioned that eq 12 can be shown[32] to be a first-order approximation to the WCA expression in eq 13.

III. Results and Discussion

A. Butane. The first of our calculations that we will discuss is on n-butane. Ryckaert and Bellemans[33,34] performed MD simulations for three different states of n-butane near the coexistence curve. In these simulations the temperature and molar volume were fixed and the compressibility factor $\beta P/\rho_m$ was calculated. For butane the monomer density ρ_m is 4 times the molecular density. In the simulations butane is modeled as a Lennard-Jones fluid with the σ and ϵ parameters chosen to match experimental data. Since the pressures chosen by Ryckaert and Bellemans to study in their simulations are near zero and the slope of the pressure volume curves is very large, a direct comparison between the simulated and calculated compressibility factors is not very meaningful. A more useful comparison, which we attempt to make here, is on the basis of the molar volume.

In Table I we show the calculated molar volumes for butane corresponding to the compressibility factors found in the simulations of Ryckaert and Bellemans. These calculations were performed using the three routes to the pressure: wall, compressibility (Comp.), and generalized

Table I. Comparison of Molar Volumes Obtained by Various Routes (Together with Barker–Henderson Perturbation Theory for the Attractive Interactions) with the Simulations of *n*-Butane by Ryckaert and Bellemans[33,34]

		$\bar{V}$ (cm³/mol)				
T (K)	$(\beta P/\rho_m)$ sim.	RB sim.	Chrg.	wall	Comp.	GFD-B
199.9[a]	0.0855	86.7	83.4	62.4	64.4	84.7
291.5[b]	0.035	99.7	147	77.4	70.7	97.9
274.0[c]	−0.138	99.5	109	69.1	67.2	91.6

[a] ϵ/k = 72 K, σ = 3.923 Å, d = 3.717 Å, l = 1.53 Å. [b] ϵ/k = 72 K, σ = 3.923 Å, d = 3.668 Å, l = 1.53 Å. [c] ϵ/k = 84 K, σ = 3.920 Å, d = 3.694 Å, l = 1.53 Å.

Flory dimer (GFD-B). The hard-sphere diameter d of the reference system was optimized using BH theory according to eq 12 using the Lennard-Jones parameters employed in the Ryckaert and Bellemans simulations. The attractive contribution to the pressure was determined from BH perturbation theory using eqs 8–10. The radial distribution function $g_0(r)$ of the reference system in eqs 9 and 12 was computed from PRISM theory for the optimized hard-core system. The different theoretical predictions in Table I (columns 4–7) differ only in the route employed to obtain the hard-chain pressure. The calculations of the charging, compressibility, and wall routes were carried out using PRISM theory for the hard-sphere contribution to the pressure, as described above and in paper 1. The calculations for the GFD-B route are described in detail in paper 1. The GFD-B route is actually a hybrid method that uses GFD computations for the hard-sphere reference system and PRISM to treat the attractions.

It can be seen from Table I that at T = 291.5 and 274.0 K the predicted molar volumes follow the pattern $\bar{V}$(Chrg.) > $\bar{V}$(GFD) > $\bar{V}$(Wall) > $\bar{V}$(Comp.), the same trend seen for the hard-sphere chains at T = 300 K shown in Figure 9 of paper 1 at fixed pressure. At the lower temperature of 199.9 K, however, the ordering of the molar volumes becomes inverted: $\bar{V}$(GFD) > $\bar{V}$(Chrg.) > $\bar{V}$(Comp.) > $\bar{V}$(Wall). This same ordering is also seen in Figure 9 of paper 1 at very high densities or packing fractions. This inversion in the ordering of the purely hard-sphere chains shifts to lower densities as the temperature is lowered. For the hard-sphere chain calculation, temperature enters the problem indirectly through the optimum hard-core diameter $d(T)$ and the intramolecular structure function $\omega(r)$.

The GFD-B calculations agree very well with the simulation molar volumes (<8%) for all three cases. In Figure 9 of paper 1 it can be observed that the charging and GFD curves are close at higher densities. Not surprisingly, the charging method also gives reasonably good agreement with the MD simulations, except at T = 291.5 K where it is 47% too high. It can be seen from Table I that the wall and compressibility routes give molar volumes that are substantially too low for butane at the simulation conditions. We conclude from this comparison with the Ryckaert–Bellemans simulation that the hybrid GFD-B route to the equation-of-state works remarkably well. It should be emphasized that no adjustable parameters were used in this comparison.

B. Polyethylene. Since Ryckaert and Bellemans[33,34] chose their Lennard-Jones parameters to match experimental data at three states, it is tempting to apply these same values to other alkane chains at other thermodynamic conditions. Unfortunately, the Lennard-Jones potential is known to be inadequate for alkanes and polyethylene.[47] As a result, the apparent Lennard-Jones parameters depend on chain length and thermodynamic state. Recently, Lopez-Rodriguez and co-workers[48] obtained the

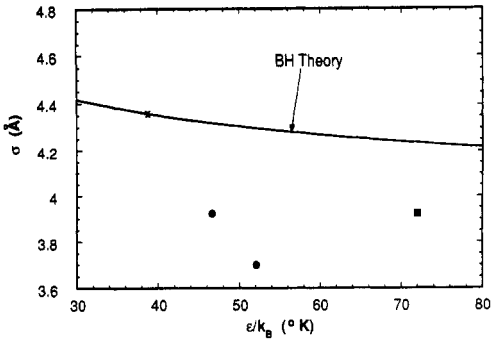

Figure 3. Lennard-Jones parameters: σ versus ϵ/k_B. The solid curve is for polyethylene (N = 6429) calculated at fixed hard-core diameter d = 3.90 Å and temperature T = 430 K, according to Barker–Henderson theory using eq 12 in the text. The filled circles correspond to parameters found by Lopez-Rodriguez and co-workers.[48] The filled square represents the value found by Ryckaert and Bellemans[33,34] for butane. The × corresponds to the parameters used in Figure 7.

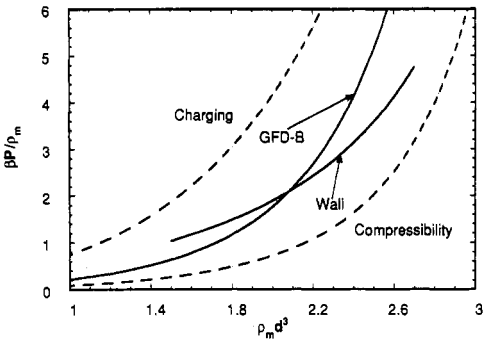

Figure 4. Hard-core equation-of-state for polyethylene (T = 430 K, N = 6429) computed by various routes.

Lennard-Jones parameters of a series of *n*-alkanes by comparing theoretical and experimental second virial coefficients. The theoretical second virial coefficients were evaluated using a two-chain Monte Carlo procedure. In this comparison, the authors allowed the well depths of methyl and methylene groups to vary independently. Interestingly, they found the ϵ parameter reflecting attractive interactions between CH_2 groups to be significantly smaller than corresponding interactions between CH_3 moieties, suggesting that the Ryckaert and Bellemans potential would not be expected to apply to polyethylene. These considerations illustrate the difficulties of unambiguously comparing theoretical and experimental equations-of-state.

In the present investigation we have tried to minimize the number of adjustable parameters to describe polyethylene by the following approach. The hard-core diameter is chosen to match the first peak in the experimental structure factor for polyethylene melts at a given temperature.[27,28,49] By this process, polyethylene at 430 K has been found[27,28,49] to have a hard-core diameter d of 3.90 Å. Such a value of d is also consistent with geometrical calculations[49] for the volume of a CH_2 group based on known atomic radii and bond lengths. By fixing d in this manner, we have an additional constraint on the acceptable Lennard-Jones parameters σ and ϵ through the Barker–Henderson relation (eq 12) or the WCA theory (eq 13). A plot of σ versus ϵ corresponding to d = 3.90 Å and satisfying eq 12 is shown in Figure 3 for polyethylene at 430 K. By choosing d from scattering experiments in this manner, we have effectively reduced the number of adjustable parameters from two to one.

Figure 4 depicts the equation-of-state of overlapping hard-sphere chains for polyethylene at 430 K (d = 3.90 Å)

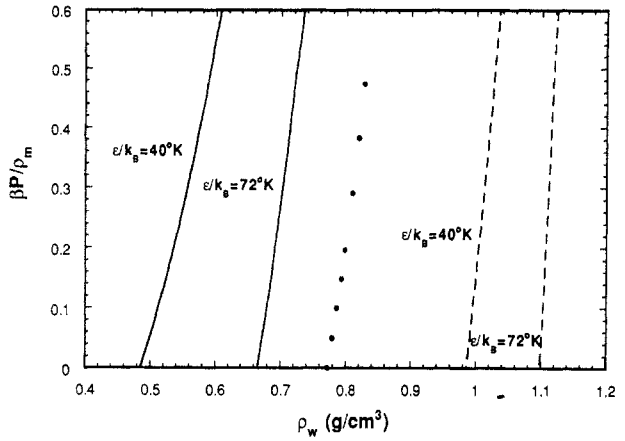

Figure 5. Equation-of-state computed for polyethylene (d = 3.90 Å, T = 430 K, N = 6429) using PRISM theory with Barker–Henderson theory. The solid curves correspond to the charging route. The dashed lines correspond to the compressibility route. The solid circles are the experimental PVT data of Olabisi and Simha.[50]

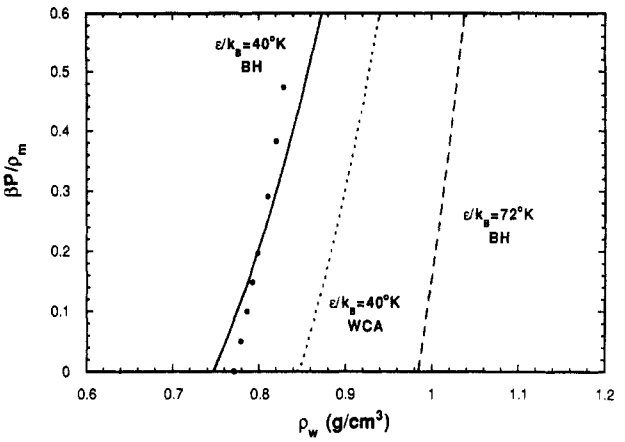

Figure 6. Equation-of-state computed for polyethylene (d = 3.90 Å, T = 430 K, N = 6429) using PRISM theory via the wall route. The solid (dashed) curve uses BH perturbation theory with ϵ/k = 40 K (72 K). For comparison, the dotted curve was calculated from WCA perturbation theory at ϵ/k = 40 K. The solid circles are the experimental PVT data of Olabisi and Simha.[50]

obtained in paper 1 using the methods discussed above. Note the wide variation in the results, depending on the route used to extract the pressure. The charging and compressibility routes bracket the GFD and wall results, in contrast to butane (see Figure 9 in paper 1), where the GFD/charging and wall/compressibility results cross at high densities.

The hard-sphere chain equations-of-state by the various routes form the basis of the reference system for the BH or WCA perturbation theory in order to treat the full Lennard-Jones potential. Because the BH approach is much easier to implement (since d depends only on temperature) than the corresponding WCA method and because the BH theory has been shown[45] to work well for molecular fluids, most of the present calculations utilize BH theory. Figure 5 displays these equation-of-state calculations at various values of the attractive well depth for the charging and compressibility routes. The points are from experimental PVT measurements[50] of Olabisi and Simha in the melt phase ($\rho_w = [23.288/d^3]\rho_m d^3$, where d is in angstroms).

The charging route, shown by the solid curves for ϵ/k_B = 40 and T = 72 K, clearly gives values of the compressibility factor in excess of the experiment at the experimental densities. Agreement with experiment would improve if ϵ/k_B was increased beyond the Ryckaert and Bellemans value of 72 K. Such an increase, however, would not seem to be justified in view of the investigation of Lopez-Rodriguez and co-workers,[48] suggesting that the interaction between methylene groups is much less than that between methyl groups. The compressibility route, shown by the dashed lines in Figure 5 for the same well depths, gives compressibility factors which are much smaller (and negative) for the experimental densities. Lowering the well depth much below 40 K is not consistent with the Lopez-Rodriguez study either, as can be seen in Figure 3. Furthermore, if ϵ/k_B is lowered to attempt to fit the experimental data, the slope of the theoretical curve will be too small. Thus, we conclude that neither the charging nor compressibility routes give satisfactory agreement with experimental PVT data on polyethylene melts at 430 K.

Figure 6 shows the calculation of the equation-of-state from the wall route. It can be seen that, for ϵ/k_B = 40 K, reasonable agreement is found with experiment, although the slope of the theoretical curve is somewhat low. The corresponding calculation using WCA theory for the

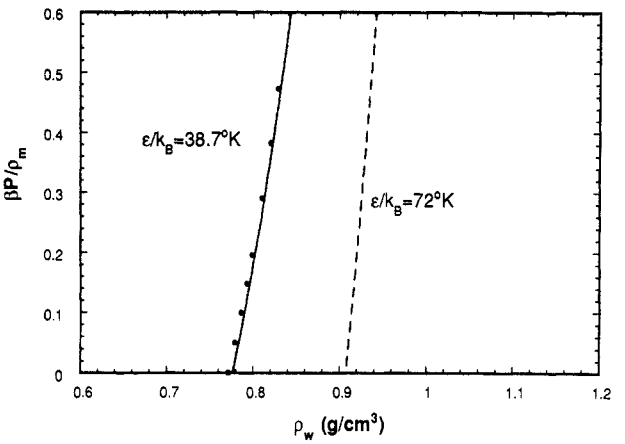

Figure 7. Equation-of-state computed for polyethylene (d = 3.90 Å, T = 430 K, N = 6429) using PRISM theory via the hybrid GFD-B approach discussed in the text. Barker–Henderson perturbation theory is used. The solid circles are the experimental PVT data of Olabisi and Simha.[50]

attractive interactions is also shown for comparison. Figure 7 depicts the hybrid GFD-B method for ϵ/k_B = 38.7 K. In this case it can be seen that the agreement with experiment at T = 430 K is almost quantitative. Furthermore, this combination of σ and ϵ indicated by the × in Figure 3 seems completely consistent with the Lopez-Rodriguez investigation.

Similar conclusions can be reached by examining the theoretical calculations at T = 500 K shown in Figure 8. These calculations were performed assuming the hard-core diameter d at 500 K remains the same (3.90 Å) as at 430 K. The well depth of ϵ/k_B = 38.7 K that fits the experiments quantitatively at 430 K leads to density predictions which are slightly high via the GFD route at 500 K. This indicates that the theoretical thermal expansion coefficient is lower than that seen in the Olabisi and Simha data. If we assume that the V–T curve is linear over the temperature range of 430–500 K, then we can estimate the thermal expansion coefficients obtained for the various routes to the equation-of-state. These estimates are shown in Table II. Note that the wall method leads to thermal expansions which are too high for polyethylene; the GFD-B route, on the other hand, is slightly lower than the Olabisi–Simha data. Unfortunately, X-ray scattering experiments have not been performed at 500 K. On the basis of previous experience,[51]

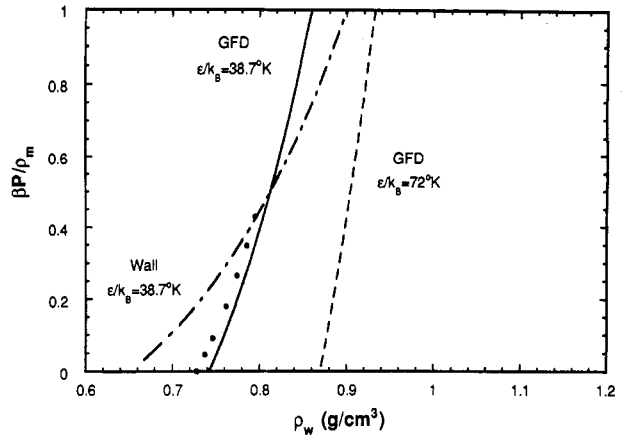

Figure 8. Equation-of-state computed for polyethylene (d = 3.90 Å, T = 500 K, N = 6429) using PRISM theory and Barker–Henderson perturbation theory. The solid circles are the experimental PVT data of Olabisi and Simha.[50]

Table II. Thermal Expansion Coefficients Estimated for the Various Routes to the Equation-of-State for Polyethylene Melts

T (K)	route	α ($\times 10^4$ K^{-1})
430–500	wall	19.0
430–500	GFD-B	6.4
430–500	exptl (Olabisi & Simha[50])	8.5

we expect that the hard-core diameter $d(T)$ which matches the first peak in the structure factor would increase slightly with temperature. Such a shift in d would increase the thermal expansion coefficient and improve the agreement with the experiments of Olabisi and Simha at 500 K. It should be pointed out that, from the BH or WCA theories, one would expect the hard-core diameter to decrease with increasing temperature, in contradiction to what we anticipate from X-ray scattering experiments. A possible explanation[51] for this reverse trend is that we represent the CH_2 groups with a united atom potential. One might anticipate that better interlocking of the hydrogens would occur as the temperature is lowered, thereby lowering the effective hard core.

IV. Conclusions

The equation-of-state of n-butane and polyethylene has been calculated from microscopic theory by four independent routes. The charging route appears to give pressures which are too high, and the compressibility route leads to pressures which are too low. This is not surprising in view of the findings from the purely hard-sphere chain calculations studied in paper 1 which shows similar trends. For polyethylene, the wall route gives much better agreement with experiment, however, the melt is calculated to be too compressible relative to experiment. An inherent difficulty in using PRISM theory (or any integral equation theory) for the reference system equation-of-state is traceable to its approximate nature. Since integral equation theories of atomic and molecular liquids are not exact, they are not thermodynamically consistent. Thus differences in the equation-of-state result from the different methods for extracting the pressure. As seen in paper 1 these differences are large in the case of polyethylene hard-sphere chains.

The hybrid GFD-B method, which uses the hard-chain GFD equation-of-state for the reference system and the radial distribution function from PRISM theory, gives remarkable agreement with both MD simulations of butane and PVT experiments on polyethylene melts. Such an approach not only takes advantage of the GFD theory which has been demonstrated to work well for hard-chain systems but also employs the PRISM theory in a mode which is known to work well for calculating the structure of the polymer liquid.

Of course, the main difficulty in making an unambiguous comparison between theory and experiment for the equation-of-state rests on our uncertain knowledge of the correct interparticle potential. Although the Lennard-Jones parameters that lead to agreement between hybrid GFD theory and experiment seem reasonable, a definitive comparison is difficult. Such uncertainties would disappear if realistic simulations of long-chain alkane systems at high density were available.

Acknowledgment. Work at Sandia National Laboratories was supported by the U.S. Department of Energy under Contract DE-AC047DP00789. Work at the University of Illinois was sponsored by the Division of Materials Sciences, Office of Basic Energy Sciences, U.S. Department of Energy. The authors thank N. J. Curro, Rice University, for performing some of the numerical equation-of-state calculations.

References and Notes

(1) Curro, J. G. *J. Macromol. Sci., Rev. Macromol. Chem.* **1974**, *C11*, 321.
(2) Simha, R.; Somcynsky, T. *Macromolecules* **1969**, *2*, 342.
(3) Sanchez, I. C.; Lacombe, R. H. *Macromolecules* **1978**, *11*, 1145.
(4) Dickman, R.; Hall, C. K. *J. Chem. Phys.* **1986**, *85*, 4108.
(5) Honnell, K. G.; Hall, C. K. *J. Chem. Phys.* **1989**, *90*, 1841.
(6) Wertheim, M. S. *J. Chem. Phys.* **1987**, *87*, 7323. Chapman, W. G.; Jackson, G.; Gubbins, K. E. *Mol. Phys.* **1988**, *65*, 1057. Chiew, P. C. *Mol. Phys.* **1990**, *70*, 129. Boublik, T.; Vega, C.; Diaz-Pena, M. *J. Chem. Phys.* **1990**, *93*, 730.
(7) Schweizer, K. S.; Curro, J. G. *J. Chem. Phys.* **1988**, *89*, 3342; *J. Chem. Phys.* **1988**, *89*, 3350.
(8) (a) Yethiraj, A.; Hall, C. K. *J. Chem. Phys.* **1991**, *95*, 8494; (b) *J. Chem. Phys.* **1991**, *95*, 1999.
(9) Schweizer, K. S.; Curro, J. G. *Phys. Rev. Lett.* **1987**, *58*, 246.
(10) Curro, J. G.; Schweizer, K. S. *Macromolecules* **1987**, *20*, 1928.
(11) Curro, J. G.; Schweizer, K. S. *J. Chem. Phys.* **1987**, *87*, 1842.
(12) Schweizer, K. S.; Curro, J. G. *Macromolecules* **1988**, *21*, 3070.
(13) Schweizer, K. S.; Curro, J. G. *Macromolecules* **1988**, *21*, 3082.
(14) Chandler, D.; Andersen, H. C. *J. Chem. Phys.* **1972**, *57*, 1930.
(15) Chandler, D. In *Studies in Statistical Mechanics VIII*; Montroll, E. W., Lebowitz, J. L., Eds.; North-Holland: Amsterdam, The Netherlands, 1982; p 274 and references cited therein.
(16) Chandler, D. *Chem. Phys. Lett.* **1987**, *140*, 108.
(17) Schweizer, K. S.; Honnell, K. G.; Curro, J. G. *J. Chem. Phys.* **1992**, *96*, 3211.
(18) Schweizer, K. S.; Curro, J. G. *Phys. Rev. Lett.* **1988**, *60*, 809.
(19) Schweizer, K. S.; Curro, J. G. *J. Chem. Phys.* **1989**, *91*, 5059.
(20) Curro, J. G.; Schweizer, K. S. *Macromolecules* **1990**, *23*, 1402.
(21) Schweizer, K. S.; Curro, J. G. *Chem. Phys.* **1990**, *149*, 105.
(22) Schweizer, K. S.; Curro, J. G. *J. Chem. Phys.* **1991**, *94*, 3986.
(23) Curro, J. G.; Schweizer, K. S. *Macromolecules* **1992**, *24*, 6737.
(24) Curro, J. G.; Schweizer, K. S; Grest, G. S.; Kremer, K. *J. Chem. Phys.* **1989**, *89*, 1357.
(25) Honnell, K. G.; Curro, J. G.; Schweizer, K. S. *Macromolecules* **1990**, *23*, 3496.
(26) Yethiraj, A.; Schweizer, K. S. *J. Chem. Phys.* **1992**, *97*, 1455. Yethiraj, A.; Hall, C. K. *J. Chem. Phys.* **1992**, *96*, 797.
(27) Honnell, K. G.; McCoy, J. D.; Curro, J. G.; Schweizer, K. S.; Narten, A.; Habenschuss, A. *J. Chem. Phys.* **1991**, *94*, 4659.
(28) Narten, A.; Habenschuss, A.; Honnell, K. G.; McCoy, J. D.; Curro, J. G.; Schweizer, K. S. *J. Chem. Soc., Faraday Trans.* **1992**, *88*, 1791.
(29) Yethiraj, A.; Hall, C. K.; Honnell, K. G. *J. Chem. Phys.* **1990**, *93*, 4553.
(30) Gao, J.; Weiner, J. H. *J. Chem. Phys.* **1989**, *91*, 3168.
(31) Yethiraj, A.; Curro, J. G.; Schweizer, K. S.; McCoy, J. D. *J. Chem. Phys.* **1993**, *98*, 1635.
(32) Hansen, J. P.; McDonald, I. R. *Theory of Simple Liquids*, 2nd ed.; Academic Press: London, 1986.
(33) Ryckaert, J. P.; Bellemans, A. *Chem. Phys. Lett.* **1975**, *30*, 123.
(34) Ryckaert, J. P.; Bellemans, A. *Faraday Discuss., Chem. Soc.* **1978**, *66*, 95.

(35) Lowden, L. J.; Chandler, D. *J. Chem. Phys.* **1974**, *61*, 5228; **1973**, *59*, 6587; **1975**, *62*, 4246.
(36) Deutch, H. P.; Binder, K. *Europhys. Lett.* **1992**, *17*, 697.
(37) Gehlsen, M. D.; Rosedale, J. H.; Bates, F. S.; Wignall, G. D.; Hansen, L.; Almadal, K. *Phys. Rev. Lett.* **1992**, *68*, 2452.
(38) Yethiraj, A.; Schweizer, K. S. *J. Chem. Phys.* **1992**, *97*, 5927.
(39) McCoy, J. D.; Honnell, K. G.; Curro, J. G.; Schweizer, K. S.; Honeycutt, J. D. *Macromolecules* **1992**, *25*, 4905.
(40) Dickman, R.; Hall, C. K. *J. Chem. Phys.* **1988**, *89*, 3168.
(41) Yethiraj, A.; Hall, C. K. *J. Chem. Phys.* **1991**, *95*, 3749.
(42) Carnahan, N. F.; Starling, K. E. *J. Chem. Phys.* **1969**, *51*, 635.
(43) Tildesey, D. J.; Streett, W. B. *Mol. Phys.* **1980**, *41*, 341.
(44) Barker, J. A.; Henderson, D. *J. Chem. Phys.* **1967**, *47*, 4714; *Annu. Rev. Phys. Chem.* **1972**, *23*, 439; *Rev. Mod. Phys.* **1976**, *48*, 587.
(45) Lombardero, M.; Abascal, J. L. F.; Lago, S. *Mol. Phys.* **1981**, *42*, 999. Abascal, J. L. F.; Martin, M.; Lombardero, M.; Vasquez, J.; Banon, A.; Santamaria, J. *J. Chem. Phys.* **1985**, *82*, 2445.
(46) Weeks, J. D.; Chandler, D.; Andersen, H. C. *J. Chem. Phys.* **1971**, *54*, 5237.
(47) Pant, P. V. K.; Boyd, R. H. *Macromolecules* **1992**, *25*, 494.
(48) Lopez-Rodriguez, A.; Vega, C.; Freire, J. J.; Lago, S. *Mol. Phys.* **1991**, *73*, 691.
(49) McCoy, J. D.; Honnell, K. G.; Schweizer, K. S.; Curro, J. G. *J. Chem. Phys.* **1991**, *95*, 9348. Slonimskii, G. L.; Askadskii, A. A.; Kitaigorodskii, A. I. *Polym., Sci. USSR* **1970**, *12*, 556.
(50) Olabisi, O.; Simha, R. *Macromolecules* **1975**, *8*, 206.
(51) Honnell, K. G.; et al., to be submitted to *J. Chem. Phys.*